JACS
JOURNAL OF THE AMERICAN CHEMICAL SOCIETY
Communication
pubs.acs.org/JACS

Catalysis of Nickel Ferrite for Photocatalytic Water Oxidation Using $[Ru(bpy)_3]^{2+}$ and $S_2O_8^{2-}$

Dachao Hong,[†] Yusuke Yamada,[†] Takaharu Nagatomi,[†] Yoshizo Takai,[†] and Shunichi Fukuzumi*[,†,‡]

[†]Department of Material and Life Science, Graduate School of Engineering, Osaka University, and ALCA, Japan Science Technology Agency (JST), Suita, Osaka 565-0871, Japan

[‡]Department of Bioinspired Science, Ewha Womans University, Seoul 120-750, Korea

Supporting Information

ABSTRACT: Single or mixed oxides of iron and nickel have been examined as catalysts in photocatalytic water oxidation using $[Ru(bpy)_3]^{2+}$ as a photosensitizer and $S_2O_8^{2-}$ as a sacrificial oxidant. The catalytic activity of nickel ferrite ($NiFe_2O_4$) is comparable to that of a catalyst containing Ir, Ru, or Co in terms of O_2 yield and O_2 evolution rate under ambient reaction conditions. $NiFe_2O_4$ also possesses robustness and ferromagnetic properties, which are beneficial for easy recovery from the solution after reaction. Water oxidation catalysis achieved by a composite of earth-abundant elements will contribute to a new approach to the design of catalysts for artificial photosynthesis.

Artificial photosynthesis that directly converts solar energy into chemical energy is one of the most promising systems for realizing a sustainable energy cycle.[1] Artificial photosynthesis systems are composed of at least three functional units; a catalyst for water oxidation ($2H_2O \rightarrow O_2 + 4H^+ + 4e^-$) to extract electrons and protons, a catalyst for reduction of protons or other chemicals to produce fuels, and light-harvesting and charge-separation molecules for solar energy harvesting and utilization.[1g] For the construction of truly sustainable systems, the use of noble or minor metals in each unit should be avoided. Photocatalytic hydrogen evolution was recently achieved with Ni nanoparticles instead of Pt nanoparticles,[2] and a long-lived charge-separated state can be established with a donor–acceptor-linked dyad that does not include metal ions.[3] On the other hand, developing efficient water oxidation catalysts (WOCs) with earth-abundant elements still remains the most challenging task for artificial photosynthesis.[4]

Most of the previously reported WOCs contain the precious metals iridium and ruthenium as active species.[5−20] Previous screening of various metal oxides suggested that cobalt oxides show relatively high activity among nonprecious metals.[15,16] Thus, much effort has been devoted to improving the catalytic activity of cobalt oxide by various methods. A distinguished example is the use of cobalt phosphate, which exhibits high catalytic activity in the electrocatalytic water oxidation.[1c] Homogeneous cobalt complexes have also been used as precursors for WOCs, which include residues derived from organic ligands during the photocatalytic water oxidation reaction.[17] Additionally, doping with trivalent metal ions such as La^{3+} has been reported to improve the catalytic activity of cobalt oxides for photocatalytic water oxidation using $[Ru(bpy)_3]^{2+}$ (bpy = 2,2′-bipyridine) as a photosensitizer and $S_2O_8^{2-}$ as a sacrificial oxidant.[18] However, foreign-metal-ion doping of iron oxides, which are much more earth-abundant than cobalt oxides, has yet to be reported for photocatalytic water oxidation.

We report herein a highly active and robust photocatalytic water oxidation catalyst composed of iron oxide doped with foreign elements. Before the iron oxide was doped with foreign metal ions, catalysis by Fe_3O_4, which contains Fe^{2+} and Fe^{3+} ions, was compared with that of Fe_2O_3, which is known as the most stable form under ambient conditions.[15] Fe_3O_4 was chosen because it is isostructural to Co_3O_4, which shows high activity in photocatalytic water oxidation.[16] Next, the Fe^{2+} ion of Fe_3O_4 was replaced by another divalent metal ion (Ni^{2+}, Mg^{2+}, or Mn^{2+}) to improve the activity and robustness of the catalyst under water oxidation conditions. In comparisons of MFe_2O_4 (M = Mg, Mn, Fe, Ni) catalysts in terms of O_2 evolution rate and O_2 yield, the highest activity for the photocatalytic water oxidation was exhibited by nickel ferrite ($NiFe_2O_4$), which has often been used for organic oxidation reactions.[21] The O_2 yields obtained usinig $NiFe_2O_4$ are comparable to those using Co_3O_4. Additionally, the ferromagnetic properties of $NiFe_2O_4$ are quite beneficial, allowing the catalyst to be recovered from the solution after the reaction using a magnet without any loss. The superior catalysis of $NiFe_2O_4$ shown in the photocatalytic water oxidation was also found in electrochemical water oxidation. The condition of the surface of $NiFe_2O_4$ after the photocatalytic water oxidation was investigated by X-ray photoelectron spectroscopy (XPS). The highly active and robust WOC composed of only the earth-abundant elements of Fe and Ni is disclosed in the photocatalytic system for the first time.

The photocatalytic water oxidation was performed in a phosphate buffer (50 mM, pH 8.0, 2.0 mL) containing a metal oxide catalyst, $Na_2S_2O_8$ (5.0 mM) as a two-electron oxidant, and $[Ru(bpy)_3]SO_4$ (0.25 mM) as a photosensitizer. The solution was purged with Ar gas for 10 min in a vial (∼1 cm i.d.) and then sealed with a rubber septum. The reaction was started by irradiating the solution with a Xe lamp (500 W) through a transmitting glass filter ($\lambda > 420$ nm) with vigorous magnetic stirring at room temperature. The overall photocatalytic cycle of water oxidation with $Na_2S_2O_8$, $[Ru(bpy)_3]SO_4$, and a WOC is depicted in Scheme 1. Photoinduced electron transfer from $[Ru(bpy)_3]^{2+*}$ (where the * denotes the excited state) to $S_2O_8^{2-}$

Received: October 3, 2012
Published: November 19, 2012

   dx.doi.org/10.1021/ja309771h | J. Am. Chem. Soc. 2012, 134, 19572−19575

Scheme 1. Cycle of Photocatalytic Water Oxidation with $Na_2S_2O_8$ and $[Ru(bpy)_3]^{2+}$ Using a Water Oxidation Catalyst

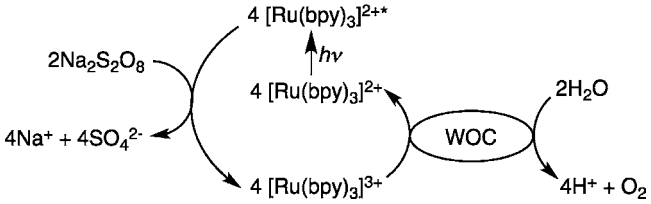

affords $[Ru(bpy)_3]^{3+}$, SO_4^{2-}, and $SO_4^{\bullet-}$. The produced $SO_4^{\bullet-}$, which is known to be a very strong oxidant [$E^0(SO_4^{\bullet-}/SO_4^{2-})$ = 2.6 V vs NHE], can oxidize another $[Ru(bpy)_3]^{2+}$ to produce 2 equiv of $[Ru(bpy)_3]^{3+}$ in the overall photoinduced process.[22] Finally, $[Ru(bpy)_3]^{3+}$ can oxidize water in the presence of the WOC to evolve O_2. However, decomposition of the photosensitizer by nucleophilic attack of OH^- or water on $[Ru(bpy)_3]^{3+}$ under neutral or basic conditions competes with electron transfer from the WOC to $[Ru(bpy)_3]^{3+}$, leading to low O_2 evolution yields.[20] Thus, highly active WOCs must improve the lifetime of the photosensitizer and the O_2 yield.

To confirm the effect of the crystal phase of the iron oxides on the catalytic activity for the photocatalytic water oxidation, Fe_2O_3 and Fe_3O_4 were synthesized by reported methods[23a,b] and characterized by powder X-ray diffraction (PXRD) measurements (Figure 1a). Co_3O_4, which is known as an active WOC, was also synthesized and characterized by PXRD as a reference.[18] All of the PXRD peaks were clearly indexed as the spinel structure for Fe_3O_4 (magnetite) and Co_3O_4 or the corundum structure for Fe_2O_3 (hematite).

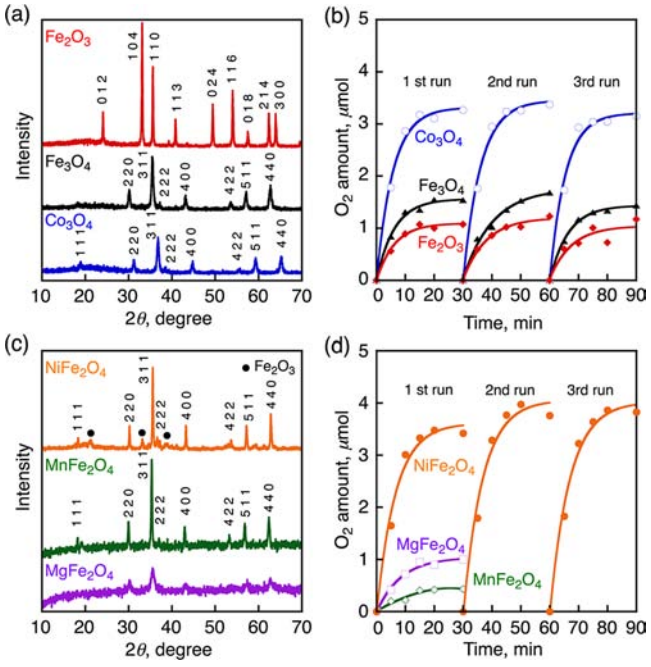

Figure 1. (a) PXRD patterns of Fe_2O_3, Fe_3O_4, and Co_3O_4. Each peak is labeled with its *hkl* index. (b) Time courses of O_2 evolution under photoirradiation (Xe lamp, $\lambda > 420$ nm) of a phosphate buffer solution (pH 8.0, 2.0 mL) containing $Na_2S_2O_8$ (5.0 mM), $[Ru(bpy)_3]SO_4$ (0.25 mM), and either Fe_2O_3, Fe_3O_4, or Co_3O_4 (0.50 g L^{-1}) at room temperature in three repetitive examinations. (c, d) Same as (a, b) but using $NiFe_2O_4$, $MgFe_2O_4$, and $MnFe_2O_4$.

Table 1. O_2 Evolution Rates (R_{O_2}) and O_2 Yields of WOCs in the Photocatalytic Water Oxidation

catalyst	R_{O_2} (μmol s^{-1} g^{-1})[a]	O_2 yield (%)[b]
$NiFe_2O_4$	5.3 ± 0.2	74 ± 4
NiO	3.0 ± 0.1	38 ± 2
Fe_2O_3	1.3 ± 0.1	21 ± 2
Fe_3O_4	1.9 ± 0.2	29 ± 3
Co_3O_4	4.8 ± 0.1	64 ± 3

[a] O_2 evolution rates (normalized by the catalyst mass) after 10 min of photoirradiation ($\lambda > 420$ nm) of an aqueous buffer solution (pH 8.0, 2 mL) containing the catalyst (0.50 g L^{-1}), $Na_2S_2O_8$ (5.0 mM), and $[Ru(bpy)_3]^{2+}$ (0.25 mM). The reported values are averages of three repetitive examinations. [b] O_2 yields, defined as twice the amount of O_2 per mole of $Na_2S_2O_8$. The reported values are averages of three repetitive examinations.

The time courses of O_2 evolution with these metal oxides are shown in Figure 1b. Table 1 tabulates the O_2 evolution rates (R_{O_2}) and O_2 yields obtained for all of the metal oxides studied. No O_2 evolution was confirmed from a reaction solution without a catalyst. The stoichiometric amount of O_2 evolution is 5.0 μmol in the present reaction systems, because $Na_2S_2O_8$ is a two-electron acceptor. A comparison between the reaction systems with iron oxides indicates that the amount of O_2 obtained after 30 min of photoirradiation with Fe_3O_4 (1.5 μmol) was larger than that with Fe_2O_3 (1.0 μmol). Even when the concentration of Fe_3O_4 was reduced to half in the reaction solution, the same amount of O_2 evolution (1.5 μmol) was achieved, with a similar O_2 evolution rate [Figure S1 in the Supporting Information (SI)]. After the first run of the photocatalytic reaction, Fe_2O_3 was recovered from the reaction solution by centrifugation for further experiments, and Fe_3O_4 was collected by a magnet. A fresh buffer solution containing $Na_2S_2O_8$ (5.0 mM) and $[Ru(bpy)_3]SO_4$ (0.25 mM) was added to the collected particles for the repetitive examination under photoirradiation. No significant change in the total amount of O_2 evolution was observed in the second and third runs from the reaction solutions with these three catalysts. These results indicate that Fe_3O_4 is a better WOC than Fe_2O_3 in the photocatalytic system. However, the catalysis by Fe_3O_4 is inferior to that by Co_3O_4 in terms of R_{O_2} and O_2 yield (i.e., the O_2 evolution of 3.2 μmol with Co_3O_4 is more than double of that with Fe_3O_4).

To improve the catalytic activity and robustness of iron-based oxides for photocatalytic water oxidation, the Fe^{2+} ions in Fe_3O_4, which are easily oxidized to Fe^{3+} under highly oxidizing conditions, were substituted with Ni^{2+}, Mg^{2+}, and Mn^{2+} while maintaining the spinel structure. A series of spinel MFe_2O_4 (M = Ni, Mg and Mn) catalysts were synthesized by reported methods[23c−e] and characterized by PXRD (Figure 1c), which confirmed the spinel structure. Figure 1d shows the time courses of O_2 evolution with $NiFe_2O_4$, $MgFe_2O_4$, and $MnFe_2O_4$ in the photocatalytic water oxidation. While the amounts of O_2 evolved from reaction solutions with $MgFe_2O_4$ (0.95 μmol) and $MnFe_2O_4$ (0.42 μmol) were smaller than that with Fe_3O_4 (1.5 μmol), the amount of O_2 evolved from the reaction solution with $NiFe_2O_4$ (3.7 μmol) was higher than that with Co_3O_4 (3.2 μmol). $NiFe_2O_4$ could be easily collected from the solution after the reaction because of its ferromagnetic properties (Figure S2). The high O_2 yield with $NiFe_2O_4$ was maintained even after the 10th run in 5 h (Figure S3). The $NiFe_2O_4$ catalyst was examined before and after the reaction by PXRD and transmission electron

dx.doi.org/10.1021/ja309771h | J. Am. Chem. Soc. 2012, 134, 19572−19575

microscopy (TEM). No significant change in either the PXRD pattern or the morphology of the $NiFe_2O_4$ catalyst was observed (Figures S4 and S5). Although the $NiFe_2O_4$ was contaminated with a small amount of Fe_2O_3, the high catalytic activity of $NiFe_2O_4$ can be ascribed to the pure $NiFe_2O_4$ because the addition of Fe_2O_3 to NiO or Fe_3O_4 showed no significant improvement in the O_2 yield (Figure S6). The catalytic activity of the MFe_2O_4 series decreased with M in the order of Ni > Fe > Mg > Mn. The catalytic activity of NiO for the photocatalytic water oxidation was also examined (Figure S7) and found to be ~1.9 μmol, which is only half that with $NiFe_2O_4$. These results clearly indicate that $NiFe_2O_4$ is a highly active and robust catalyst for the photocatalytic water oxidation.

As the catalytic activities of heterogeneous catalysts are usually compared after normalization by the specific surface area, the R_{O_2} values calculated from the initial slopes (10 min) of the time courses were normalized by the Brunauer–Emmett–Teller surface areas determined by N_2 adsorption measurements at 77 K (48 $m^2\ g^{-1}$ for $NiFe_2O_4$, 45 $m^2\ g^{-1}$ for Fe_3O_4, 34 $m^2\ g^{-1}$ for Co_3O_4, and 150 $m^2\ g^{-1}$ for NiO) to obtain apparent turnover frequencies (TOFs). The apparent TOF of 0.11 μmol $s^{-1}\ m^{-2}$ obtained with $NiFe_2O_4$ was higher than those with Fe_3O_4 (0.042 μmol $s^{-1}\ m^{-2}$) and NiO (0.020 μmol $s^{-1}\ m^{-2}$). These results indicate that the high activity of $NiFe_2O_4$ results from the composite effect of nickel and iron oxides. The apparent TOF with $NiFe_2O_4$ is slightly smaller than that with Co_3O_4 (0.14 μmol $s^{-1}\ m^{-2}$). However, the O_2 yield obtained with $NiFe_2O_4$ (74%) was higher than that with Co_3O_4 (64%) by 10%. The O_2 yield with $NiFe_2O_4$ is also higher than those reported for catalysts containing precious metals such as IrO_2 particles (69%, pH 5.0)[15] and RuO_2 particles (22%, pH 5.0)[15] and abundant elements such as Mn_xO_y particles (55%, pH 5.8)[19] and comparable to that with $LaCoO_3$ particles (74%, pH 7.0).[18] Thus, $NiFe_2O_4$ composed of earth-abundant elements is one of most active catalysts for the photocatalytic water oxidation.

The superior catalysis of $NiFe_2O_4$ for the photocatalytic water oxidation was scrutinized under electrocatalytic conditions. The electrochemical deposition of nickel or cobalt on the surface of hematite Fe_2O_3 has previously been reported to improve the catalysis of electrochemical water oxidation by Fe_2O_3.[24,25] Figure 2 shows cyclic voltammograms (CVs) of water using a working electrode modified with a metal oxide catalyst in a pH 8.0 buffer solution. The anodic currents with $NiFe_2O_4$ started growing at ~0.8 V vs SCE and reached more than 650 μA at 1.5 V vs SCE, which is larger than those with iron-based oxides. The overpotential of $NiFe_2O_4$ for the electrochemical water oxidation (η = 0.43 V) is comparable to the reported overpotentials of catalysts such as cobalt phosphate,[1c] CoO_x,[26] and nickel borate[27] (Table S1 in the SI). At ~0.8 V, a small redox couple assignable to the redox of Ni^{2+} species appears. A similar redox couple has been assigned to Ni^{2+}/Ni^{3+} for a nickel oxide electrode formed on Ni in alkaline solution.[28] Recently, the oxidized nickel species at anodic potentials has been assigned as Ni^{4+} in nickel borate by X-ray absorption near-edge structure spectra.[27] Further investigation is necessary to clarify the valence of the active nickel species of $NiFe_2O_4$, but the growth of this oxidation peak ensures that a high-valent nickel species is an active species for the water oxidation. The onset potentials for water oxidation with both Fe_2O_3 and Fe_3O_4 were observed at ~1.1 V. The anodic currents with Fe_2O_3 and Fe_3O_4 at 1.5 V were as small as 190 and 290 μA, respectively. These results suggest that incorporation of Ni^{2+} ions enhances the water oxidation ability of iron oxides, which can exhibit high activity for photocatalytic water oxidation.

A critical issue for a series of spinel compounds under highly oxidizing conditions is oxidation of divalent metal species. The oxidation may lead to microphase separation and deactivation of the catalyst. It has been reported that magnetite Fe_3O_4 is oxidized to form Fe_2O_3 under highly oxidizing conditions.[29] NiO is rather stable, but its transformation to nonstoichiometric nickel oxide under highly oxidizing conditions has been reported.[30] Thus, confirmation of the surface conditions of each component after water oxidation was necessary. The change in the surface conditions of $NiFe_2O_4$ before and after the photocatalytic reaction was observed by XPS, which was performed in the Fe $2p_{3/2}$, Ni $2p_{3/2}$, O 1s, Ru 3d, and C 1s energy regions. No peak was observed in the Ru 3d region. The binding energy of each element was corrected using the C 1s peak from residual carbon (284.8 eV). Figure 3a displays the XPS spectra for the Ni $2p_{3/2}$ peak at 854.8 eV with a weak satellite peak at 861 eV for $NiFe_2O_4$ samples before and after the reaction. The binding energies of these peaks indicate that the Ni species in the samples are Ni^{2+} by comparison with the Ni $2p_{3/2}$ peak positions of Ni metal and NiO (Figure S8a). The similar intensity ratios for the main and satellite peaks for the two samples indicate that the surface conditions were the same even after the photocatalytic water

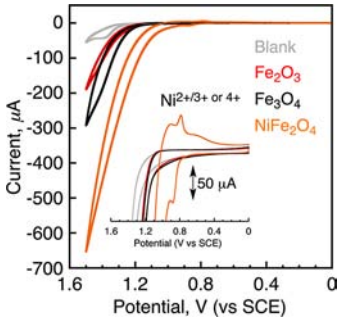

Figure 2. CVs in a buffer solution (pH 8.0) with a carbon paste working electrode (A = 0.071 cm^2) containing no metal oxide (gray), 5% $NiFe_2O_4$ (orange), Fe_3O_4 (black), or Fe_2O_3 (red) (standard calomel electrode; Pt wire counter electrode; scan rate 100 mV s^{-1}). The inset shows the initial range of the electrocatalytic current.

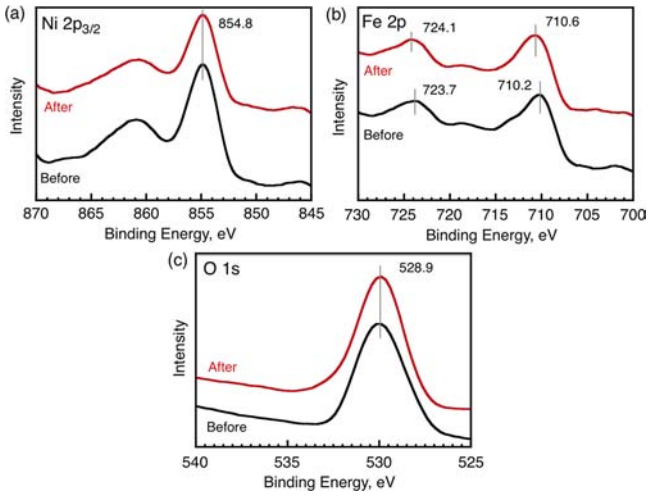

Figure 3. XPS spectra of $NiFe_2O_4$ before and after the reaction in the (a) Ni $2p_{3/2}$, (b) Fe 2p, and (c) O 1s energy regions.

dx.doi.org/10.1021/ja309771h | J. Am. Chem. Soc. 2012, 134, 19572–19575

oxidation was performed under highly oxidizing conditions. Figure 3b displays the XPS spectrum for the Fe $2p_{3/2}$ peak at 710.2 eV with a weak satellite peak at 723.7 eV for $NiFe_2O_4$ before the reaction and that at 710.6 eV with a weak satellite peak at 724.1 eV after the reaction. These peaks are assigned to Fe^{3+} by comparison with the Fe $2p_{3/2}$ peaks of Fe_2O_3 and Fe metal (Figure S8b). Although the main Fe $2p_{3/2}$ peak from the sample after the reaction was slightly shifted in the direction of higher binding energy, the same separation between the main and satellite peaks in the two samples and the similarity of the peak shapes, including the satellite peaks, over the whole energy region between 700 and 730 eV strongly indicate that there was no change in the valence state of Fe^{3+}. The absence of changes in the surface conditions of $NiFe_2O_4$ before and after the reaction was also supported by the absence of a shift in the O 1s peak (Figure 3c). Thus, $NiFe_2O_4$ is highly robust even during the photocatalytic water oxidation.

In summary, we have demonstrated for the first time superior catalysis of photocatalytic water oxidation by a material composed of only earth-abundant elements, $NiFe_2O_4$. This catalyst possesses high catalytic activity as well as durability in photocatalytic water oxidation with $Na_2S_2O_8$ and $[Ru(bpy)_3]^{2+}$, as evidenced by the maintenance of a high O_2 yield after 10 repeated uses. Cyclic voltammetry studies of electrocatalytic water oxidation with $NiFe_2O_4$ suggested that a high-valent nickel species is the active species for the photocatalytic water oxidation. This has important implications for the exploitation of efficient WOCs to expand the use of iron-based oxides for water oxidation.

■ ASSOCIATED CONTENT

Supporting Information

Experimental section, time courses of O_2 evolution under different conditions, photograph of $NiFe_2O_4$ attracted by a magnet, comparison of overpotentials, PXRD patterns, TEM images, and XPS spectra. This material is available free of charge via the Internet at http://pubs.acs.org.

■ AUTHOR INFORMATION

Corresponding Author

fukuzumi@chem.eng.osaka-u.ac.jp

Notes

The authors declare no competing financial interest.

■ ACKNOWLEDGMENTS

This work was partially supported by Grants-in-Aid (20108010 and 24350069) from MEXT (Japan) and by NRF/MEST (Korea) through the WCU (R31-2008-000-10010-0) and GRL (2010-00353) Programs (to S.F.). We acknowledge Research Centre for Ultra-Precision Science & Technology for TEM measurements and Prof. Norimitsu Tohnai at OU for XRD measurements.

■ REFERENCES

(1) (a) Lewis, N. S.; Nocera, D. G. *Proc. Natl. Acad. Sci. U.S.A.* **2006**, *103*, 15729. (b) Eisenberg, R.; Gray, H. B. *Inorg. Chem.* **2008**, *47*, 1697. (c) Kanan, M. W.; Nocera, D. G. *Science* **2008**, *321*, 1072. (d) Youngblood, W. J.; Lee, S.-H. A.; Maeda, K.; Mallouk, T. E. *Acc. Chem. Res.* **2009**, *42*, 1966. (e) Concepcion, J. J.; Jurss, J. W.; Brennaman, M. K.; Hoertz, P. G.; Patrocinio, A. O. T.; Murakami Iha, N. Y.; Templeton, J. L.; Meyer, T. J. *Acc. Chem. Res.* **2009**, *42*, 1954. (f) Romain, S.; Vigara, L.; Llobet, A. *Acc. Chem. Res.* **2009**, *42*, 1944. (g) Fukuzumi, S. *Eur. J. Inorg. Chem.* **2008**, 1351.

(2) Yamada, Y.; Miyahigashi, T.; Kotani, H.; Ohkubo, K.; Fukuzumi, S. *Energy Environ. Sci.* **2012**, *5*, 6111.

(3) (a) Fukuzumi, S.; Kotani, H.; Ohkubo, K.; Ogo, S.; Tkachenko, N. V.; Lemmetyinen, H. *J. Am. Chem. Soc.* **2004**, *126*, 1600. (b) Hoshino, M.; Uekusa, H.; Tomita, A.; Koshihara, S.; Sato, T.; Nozawa, S.; Adachi, S.; Ohkubo, K.; Kotani, H.; Fukuzumi, S. *J. Am. Chem. Soc.* **2012**, *134*, 4569. (c) Kotani, H.; Ohkubo, K.; Fukuzumi, S. *Faraday Discuss.* **2012**, *155*, 89.

(4) Du, P.; Eisenberg, R. *Energy Environ. Sci.* **2012**, *5*, 6012.

(5) Najafpour, M. M.; Ehrenberg, T.; Wiechen, M.; Kurz, P. *Angew. Chem., Int. Ed.* **2010**, *49*, 2233.

(6) Fillol, J. L.; Codolà, Z.; Garcia-Bosch, I.; Gómez, L.; Pla, J. J.; Costas, M. *Nat. Chem.* **2011**, *3*, 807.

(7) Yin, Q. S.; Tan, J. M.; Besson, C.; Geletii, Y. V.; Musaev, D. G.; Kuznetsov, A. E.; Luo, Z.; Hardcastle, K. I.; Hill, C. L. *Science* **2010**, *328*, 342.

(8) Murakami, M.; Hong, D.; Suenobu, T.; Yamaguchi, S.; Ogura, T.; Fukuzumi, S. *J. Am. Chem. Soc.* **2011**, *133*, 11605.

(9) Poulsen, A. K.; Rompel, A.; McKenzie, C. J. *Angew. Chem., Int. Ed.* **2005**, *44*, 6916.

(10) Polyansky, D. E.; Muckerman, J. T.; Rochford, J.; Zong, R.; Thummel, R. P.; Fujita, E. *J. Am. Chem. Soc.* **2011**, *133*, 14649.

(11) Duan, L.; Bozoglian, F.; Mandal, S.; Stewart, B.; Privalov, T.; Llobet, A.; Sun, L. *Nat. Chem.* **2012**, *4*, 418.

(12) Fukuzumi, S.; Kato, S.; Suenobu, T. *Phys. Chem. Chem. Phys.* **2011**, *13*, 17960.

(13) Kaveevivitchai, N.; Chitta, R.; Zong, R.; El Ojaimi, M.; Thummel, R. P. *J. Am. Chem. Soc.* **2012**, *134*, 10721.

(14) Hong, D.; Murakami, M.; Yamada, Y.; Fukuzumi, S. *Energy Environ. Sci.* **2012**, *5*, 5708.

(15) Harriman, A.; Pickering, I. J.; Thomas, J. M.; Christensen, P. A. *J. Chem. Soc., Faraday Trans. 1* **1988**, *84*, 2795.

(16) Jiao, F.; Frei, H. *Energy Environ. Sci.* **2010**, *3*, 1018.

(17) Hong, D.; Jung, J.; Park, J.; Yamada, Y.; Suenobu, T.; Lee, Y.-M.; Nam, W.; Fukuzumi, S. *Energy Environ. Sci.* **2012**, *5*, 7606.

(18) Yamada, Y.; Yano, K.; Hong, D.; Fukuzumi, S. *Phys. Chem. Chem. Phys.* **2012**, *14*, 5753.

(19) Jiao, F.; Frei, H. *Chem. Commun.* **2010**, *46*, 2920.

(20) Morris, N. D.; Mallouk, T. E. *J. Am. Chem. Soc.* **2002**, *124*, 11114.

(21) (a) Fouad, O. A.; Abdel, H. K. S.; Rashad, M. M. *Top. Catal.* **2008**, *47*, 61. (b) Miki, J.; Asanuma, M.; Tachibana, Y.; Shikada, T. *J. Catal.* **1995**, *151*, 323. (c) Turek, W.; Strzezik, J.; Krowiak, A. *React. Kinet. Mech. Catal.* **2012**, *107*, 115.

(22) Kaledin, A. L.; Huang, Z.; Geletii, Y. V.; Lian, T.; Hill, C. L.; Musaev, D. G. *J. Phys. Chem. A* **2010**, *114*, 73.

(23) (a) Elizarova, G. L.; Matvienko, L. G.; Parmon, V. N. *J. Mol. Catal.* **1987**, *43*, 171. (b) Wang, L.; Li, J.; Jiang, Q.; Zhao, L. *Dalton Trans.* **2012**, *41*, 4544. (c) Cheng, Y.; Zheng, Y.; Wang, Y.; Bao, F.; Qin, Y. *J. Solid State Chem.* **2005**, *178*, 2394. (d) Deng, H.; Chen, H.; Li, H. *Mater. Chem. Phys.* **2007**, *101*, 509. (e) Wang, L.; Li, J.; Wang, Y.; Zhao, L.; Jiang, Q. *Chem. Eng. J.* **2012**, *181*−*182*, 72.

(24) (a) Liao, P.; Keith, J. A.; Carter, E. A. *J. Am. Chem. Soc.* **2012**, *134*, 13296. (b) Landon, J.; Demeter, E.; Inoglu, N.; Keturakis, C.; Wachs, I. E.; Vasic, R.; Frenkel, A. I.; Kitchin, J. R. *ACS Catal.* **2012**, *2*, 1793.

(25) Liu, Y.; Yu, Y.-X.; Zhang, W.-D. *Electrochim. Acta* **2012**, *59*, 121.

(26) Stracke, J. J.; Finke, R. G. *J. Am. Chem. Soc.* **2011**, *133*, 14872.

(27) Bediako, D. K.; Lassalle-Kaiser, B.; Surendranath, Y.; Yano, J.; Yachandra, V. K.; Nocera, D. G. *J. Am. Chem. Soc.* **2012**, *134*, 6801.

(28) Lyons, M. E. G.; Brandon, M. P. *Int. J. Electrochem. Sci.* **2007**, *3*, 1386.

(29) Tang, J.; Myers, M.; Bosnick, K. A.; Brus, L. E. *J. Phys. Chem. B* **2003**, *107*, 7501.

(30) Greenwood, N. N.; Earnshaw, A. *Chemistry of the Elements*, 2nd ed.; Butterworth−Heinemann: Oxford, U.K., 1997.